EIF4A3 Acts on the PI3K–AKT–ERK1/2–P70S6K Pathway through FLOT1 to Influence the Development of Lung Adenocarcinoma

Wenhao Yu[1], Jinghui Liang[2], Tao Fang[1], Jin Jiang[1], Renchang Zhao[1], Rongyang Li[1], Jingyi Han[1], and Hui Tian[1]

ABSTRACT

Lung adenocarcinoma (LUAD) is a major lung cancer subtype. In this study, we discovered that the eukaryotic translation initiation factor EIF4A3 expression was significantly higher in LUAD tissues and that this higher expression was closely linked to a poor prognosis for LUAD. In addition, we demonstrated that the knockdown of EIF4A3 significantly inhibited the proliferation, invasion, and migration of LUAD cells *in vitro* and *in vivo*. The findings of mass spectrometry analysis revealed that EIF4A3 could interact with Flotillin-1 in LUAD cells and that EIF4A3 could positively regulate the expression of FLOT1 at the protein level. Meanwhile, transcriptome sequencing showed that EIF4A3 could influence the development of LUAD by affecting PI3K–AKT–ERK1/2–P70S6K and PI3K class III–mediated autophagy in the Apelin pathway. In addition, we confirmed that Flotillin-1 expression was upregulated in LUAD based on the existing literature, and knockdown of FLOT1 could inhibit the proliferation and migration of LUAD cells. In addition, the knockdown of Flotillin-1 reversed the increase of cell proliferation and migration caused by EIF4A3 overexpression. Furthermore, we found that the activation of PI3K–AKT–ERK1/2–P70S6K signaling pathway and PI3K class III–mediated autophagy caused by EIF4A3 overexpression was rescued by the knockdown of FLOT1. In a word, we proved that EIF4A3 positively regulates the expression of FLOT1 and plays a procancer role in LUAD.

Implications: Our study revealed the role of EIF4A3 in prognosis and tumor progression in LUAD, indicating that EIF4A3 could be used as the molecular diagnostic and prognostic therapeutic target.

Introduction

Lung cancer is still the most common cause of death, and the incidence and mortality of lung cancer is rising (1). The most common subtype of lung cancer is lung adenocarcinoma (LUAD) worldwide (2). Lung cancer treatment options include surgical procedures, radiotherapy, chemotherapy, and targeted therapy (3). Despite breakthroughs in detection and therapy over the past quarter-century, the prognosis for people with lung cancer remains grim. Except for the most localized cancers, response to current standard therapies is poor (4). In contrast, molecular targeted therapies and immunotherapies have significantly altered the treatment paradigm for lung cancer, and they have the advantage of significantly improving patient prognosis; therefore, it is of great clinical importance for us to find new molecular targets for the treatment of lung cancer (5, 6).

The malignant phenotype of tumors is essentially the product of aberrant gene expression. Among others, oncogenic mRNAs are upregulated by translational expression, and it has been found that such mRNAs contain longer and more structurally complex 5′-UTRs, which also require high amounts of eukaryotic initiation factor 4A (EIF4A) helicase activity for effective translation (7). At the same time, much of the regulation of translation is targeted to the initiation phase, and more specifically, the ribosome recruitment phase requires the 40S ribosome (and associated factors) that the eukaryotic initiation factor (EIF) 4F complex enters to prepare the mRNA, this complex is composed of the EIF4E cap-binding protein, the EIF4G scaffolding protein, and the EIF4A RNA helicase, which is the only enzyme in the EIF4F complex. Because many of the common signaling pathway abnormalities found in cancer affect protein synthesis, the search for factors affecting the translation initiation phase is a viable antitumor strategy, especially for EIF4A, the enzymatic subunit of the EIF4F complex, which has been widely explored as an available molecular target. In summary, cancer therapy with EIF4A as a molecular target is becoming a research focus (8, 9).

The protein structures of the EIF4A family share common features. As typical members of DEAD-box helicases, EIF4A proteins possess two RecA-like structural domains with a flexible central hinge region that allows them to switch between open and closed conformations, whereas they both have nine conserved structural domains containing ATPase and RNA helicase activities. EIF4A, therefore, plays a significant function in the mRNA cap-dependent translation initiation phase. Because cancer cell signaling pathways are primarily focused on cap-dependent translation, EIF4A is highly expressed and plays a crucial role in a variety of malignancies (10).

EIF4A3, a nuclear matrix protein and an exon junction complex (EJC) component, belongs to the EIF4A family of proteins. EIF4A3 engages in posttranscriptional gene regulation under physiologic conditions via enhancing EJC regulation of precursor mRNA splicing, thereby affecting certain mRNA decay (11). EIF4A3 has been reported to be intimately linked to the evolution of a range of malignancies containing breast cancer (12, 13), prostate cancer (14), glioblastoma (15), colorectal cancer (16), and ovarian cancer (17). In LUAD, it has been reported in the literature that EIF4A3 can act as an RNA-binding protein that binds to a variety of RNAs to exert pro-oncogenic

[1]Department of Thoracic Surgery, Qilu Hospital of Shandong University, Jinan, Shandong, China. [2]The Wistar Institute, Philadelphia, Pennsylvania.

Corresponding Author: Hui Tian, Department of Thoracic surgery, Qilu Hospital of Shandong University, Jinan, 250012, China. Phone/Fax: 8618-5600-80016; E-mail: tianhuiql@email.sdu.edu.cn

Mol Cancer Res 2023;21:713–25

doi: 10.1158/1541-7786.MCR-22-0984

effects (18). However, no studies have yet confirmed that it can interact with other proteins to influence the development of lung cancer. At the same time, the molecular mechanism of action of EIF4A3 itself in lung cancer is not well studied. Here, for the first time, we investigated the molecular mechanism of action of the proto-oncogene EIF4A3 in LUAD and the downstream target genes it can bind in this study. Therefore, our study can also provide a new selective therapeutic target for the clinical treatment of LUAD and can also contribute to improving patient prognosis.

Material and Methods

Clinical samples

The tissue microarray of LUAD tissues (HLugA180Su08) was obtained from Shanghai Outdo Biotech Company. It contains 89 LUAD tissues and 81 adjacent noncancerous tissues including the gender, age, clinical stage, and survival information of each patient. The Ethics Committee of Shanghai Outdo Biotech Company approved this study (No. SHYJS-CP-1904014). We collected 10 paired LUAD tissues and adjacent tissues for Western blotting. At Qilu Hospital (Jinan, China), surgical removal of LUAD and paraneoplastic tumor tissue from LUAD patients between 2020 and 2021. Pathology examined all diagnoses. Research Ethics Committee of Qilu Hospital, Shandong University approved this study (KYLL-2021-1053). All aspects of the study conformed to the standards set forth in the Declaration of Helsinki and informed consent was obtained from patients for all patient studies.

Cell culture and treatment

The Chinese Academy of Sciences' Shanghai Cell Bank Research Center provided the HBE, A549, H1299, PC9, BEAS-2B, and H1975 LUAD cell lines. Cell lines were grown in RPMI-1640 media (Gibco) and Dulbecco's Modified Eagle Medium (Gibco), in a humidified incubator with 5% CO_2 at 37°C. All media were formulated with the addition of 10% fetal bovine serum (FBS; Gibco). Cells were certified to be analyzed every 3 to 6 months using short tandem repeat, whereas cells are monitored every 3 months using the MycoAlert Mycoplasma Detection Kit (Lonza). PC9, H1299, and A549 cell lines were authenticated by Beijing Tsingke Biotech Co., Ltd. on September 17, 2021. The experiment was generally carried out 1 week after the cells were thawed. For repetitive experiments, cells are cultured for a maximum of two months. The Sh-NC and Sh-EIF4A3 lentiviruses (Genecopia Co.) were transfected into PC9 stable cells (MOI:20) and H1299 stable cells (MOI:10), whereas the EIF4A3 overexpression lentiviruses (Jikai Co.) were transfected in A549 stable cells (MOI:20). The puromycin was used to select the transfected cells for 7 days. GenePharma Co., Ltd. supplied both the siRNA-Flotillin1 and its corresponding negative control. And we carried out transient transfection of cells with siRNAs utilizing jetPRIME transfection reagent (Polyplus) in accordance with the instructions. Then we performed subsequent experiments after 48 to 72 hours of transfection. The si-RNA sequences are provided in Supplementary Table S1.

Western blotting

To extract their proteins, cells and LUAD samples were lysed in RIPA buffer (Beyotime). Proteins were separated using a 10% or 12% SDS-PAGE gel and then electrically transported to a polyvinylidene difluoride membrane, which was blocked for 1 hour with 5% nonfat milk to prevent nonspecific antibody binding prior to being treated with primary antibodies (Supplementary Table S2) at 4°C overnight. The membranes were detected with an enhanced chemiluminescence (ECL) system following incubation with corresponding secondary antibodies.

Cell counting kit-8 cell proliferation assay

96-well plates were inoculated with transduced cells and cultivated for 24, 48, 72, and 96 hours. The Cell Counting Kit-8 (CCK8; APExBIO, #K1018) was added into the cells, and after 2 hours of incubation in the dark, absorbance was measured at 450 nm using a microplate reader. The assay was performed three independent times.

EDU assay

96-well plates were inoculated with transduced cells and cultured overnight. After that, Edu staining was conducted as instructed using the Edu *In Vitro* Kit. Finally, fluorescence microscopy was used to photograph the labeled cells. The experiment was conducted three times independently.

Colony formation assay

In six-well plates, H1299, A549, and PC9 cells were seeded. After 14 days of cultivation, the cells were fixed for 30 minutes in 4% paraformaldehyde and stained for 20 minutes with crystal violet. We then washed the cells thrice and then calculated the number of colony formation, which was conducted three times independently.

Wound-healing assay

The infected cells were spread across 6-well plates until their growth was complete. Subsequently, draw a straight line on the cell with the tip of a 10-μm pipette. Serum-free media were substituted for the medium after three PBS washes. The wound's width was then inspected and measured under a microscope at 0 and 24 hours. The experiment was conducted three times independently.

Transwell assay

The infected cells were introduced without Matrigel to the upper transwell chamber, and the lower transwell chamber received 700 μL of culture media containing 20% FBS. 24 hours later, the lowest chamber's cells were fixed for 30 minutes and then stained for 20 minutes, and photographs were taken with a microscope. The experiment was conducted three times independently.

Immunoprecipitation (IP) assay

In IP buffer (P0013, Beyotime), PC9 and H1299 cells were lysed. Then, we took out a certain amount of proteins from them as input group and an appropriate amount of the protein lysates was mixed with 2ug antibodies against EIF4A3 (ET7108–11, HUABIO, China) or Flotillin-1 (12271-1-AP, Proteintech) and IgG (ab172730, Abcam) at 4°C for 1 hour on a rotating device. Then, 30 μL of protein A/G plus agarose was added to the mixture, which was then incubated overnight at 4°C on the rotating apparatus. The next day, we washed the mixture 5 times with IP buffer and the precipitated proteins were mixed with loading buffer for western blot analysis. At last, we performed western blotting to detect the expression of EIF4A3 and Flotillin-1.

In vivo experiments

Weitonglihua animal company provided the 4-week-old BALB/c nude mice to us. Ten nude mice were allocated at random between two groups to create the xenograft tumor model. Then, transduced PC9 (LV-sh-EIF4A3 and LV-sh-negative control) cells were inserted

hypodermically in the right axillary area of each mouse. Every 5 days, the size of the tumors was measured. The volume of the tumor was calculated using the following formula: $V = (\text{length} \times \text{width2})/2$. And after 28 days, each tumor was gathered and weighed.

For the experimental model for lung metastasis, we injected into the 10 nude mice, which were separated into two groups at random, with infected cells via the tail vein. After 2 months, we used live nude mice and their livers and lungs after execution to shoot live imaging. The Medical Ethics Committee of Shandong University's Qilu Hospital approved and supervised all of the experiments.

IHC analysis

4% paraformaldehyde was used to fix LUAD tissue and mouse tumor tissue. After incubation at 60°C for 1 hour, dewaxing, and rehydrating the sample, antigen was extracted using citrate buffer at 97°C for 20 minutes. Peroxidase blockers were used for 10 minutes at room temperature. After incubating with 5% normal goat serum in PBST for 2 hours at 37°C, the slides were incubated overnight at 4°C with primary antibodies against EIF4A3 and Ki67. Before restaining with hematoxylin, each slide was treated with an HRP-labeled secondary antibody, and the signal was developed using DAB solution after three washes with TBST. And the slides were captured using an inverted microscope.

Transcriptomic sequencing, protein characterization mass spectrometry, and bioinformatics analysis

Transcriptomic sequencing was carried out by LC Bio-Technology Co., Ltd. The mRNA transcripts were identified by sequencing the transcriptome which expressed differently in EIF4A3 knockdown PC9 cells than in control PC9 cells. The KEGG pathway enrichment was drawn based on the OmicStudio platform (https://www.omicstudio.cn/tool).

Mass spectrometry was performed by Jikai Co. We performed immunoprecipitation followed by the collection of precipitated beads after centrifugation for mass spectrometry analysis. It was used to investigate what protein is the component that interacts with EIF4A3.

Gene-expression information was obtained from TCGA data sets (https://xenabrowser.net/) of LUAD patients, whereas gene-expression data from LUAD patients were downloaded from GEO data sets using GSE 10072 (https://www.ncbi.nlm.nih.gov/gds).

TEM imaging

H1299, PC9, and A549 cell line–transfected associated viruses were digested using trypsin, collected by centrifugation, resuspended by adding 0.5% glutaraldehyde fixative for 10 minutes, centrifuged again and fixed by adding 3% glutaraldehyde. Finally, cell samples were refixed with 1% osmium tetroxide, dehydrated step by step in acetone, Ep812 embedding. Samples were stained accordingly and then cut with a diamond knife. Using a JEM-1400-FLASH transmission electron microscope, sections were inspected.

Statistical analysis

All statistical analyses were carried out using GraphPad Prism Software. Each experiment was conducted at least three times independently. All data were presented as mean ± standard deviation (SD). As specified, the log-rank test, Kaplan–Meier survival analysis, Pearson Chi-square test, two-tailed Student *t* test, Fisher exact test, and Pearson correlation analysis were conducted for comparisons. Using one-way ANOVA, the differences between three or more groups were compared.

Results

EIF4A3 is highly elevated in LUAD tissues widely and is associated with a poor prognosis in patients with LUAD

First, we explored the role of EIF4A3 in LUAD, and we carried out the bioinformatics analysis using the GEO LUAD databases (GSE10072) and TCGA LUAD database. Results demonstrated that EIF4A3 expression was increased in LUAD tissues than in normal tissues (**Fig. 1A** and **B**). Subsequently, IHC staining was used to ascertain EIF4A3 protein expression in 89 cancer tissues and 81 paraneoplastic tissues (**Fig. 1C**). IHC score showed that the expression of EIF4A3 was upregulated in LUAD tissues (**Fig. 1D**). At the same time, we used western blotting to find that EIF4A3 protein expression is higher in 10 malignant tissues than in paired normal noncancerous tissues (**Fig. 1E**).

Then, we examined the relationship between certain pathologic indicators and EIF4A3 expression in clinical patients with LUAD. According to the chi-square test, the EIF4A3 protein expression level was significantly associated with age ($P = 0.016$), tumor size ($P = 0.018$), T-stage ($P < 0.001$), and TNM stage ($P = 0.030$) but not with gender and grade (Supplementary Table S3). According to the Kaplan–Meier survival analysis, high EIF4A3 protein expression was significantly linked to poor prognosis in LUAD (**Fig. 1F**). Similarly, our online analysis using the Kaplan–Meier Plotter online website showed that higher EIF4A3 expression appeared to be associated with a shorter OS compared with lower EIF4A3 expression (Supplementary Fig. S1A). Overall, our results confirmed the cancer-promoting role of EIF4A3 in LUAD.

EIF4A3 promotes the proliferation and migration of LUAD cells *in vitro*

Using western blotting, we found that the H1299 and PC9 cell lines had higher-level expression and the A549 cell line had lower-level expression (Supplementary Fig. S1B). After verifying the knockdown efficiency of three small interfering sequences in H1299 and PC9, we selected the most efficient sequence for lentivirus design (Supplementary Fig. S1C). Then we constructed the PC9 and H1299 cell lines with the stable knockdown expression of EIF4A3 and the A549 cell line with stable overexpression of EIF4A3 to perform follow-up experiments. With CCK-8 assay, EdU assay, and colony formation, we found that compared with controls, EIF4A3 knockdown resulted in slower tumor cell appreciation, whereas overexpression of EIF4A3 leads to an accelerated rate of tumor cell appreciation (**Fig. 2A–C**). Besides, with the transwell assay and wound-healing assay, we found that the number of the migrated cells and the area of the wound healing were decreased after EIF4A3 knockdown, whereas they were increased in the EIF4A3 overexpression A549 cell lines (**Fig. 2D–F**). These results indicated that EIF4A3 could increase the proliferation and migration of LUAD cells.

EIF4A3 silencing decreased LUAD cells proliferation, invasion, and migration *in vivo*

Subsequently, to investigate how EIF4A3 affects tumor development and migration, we conducted *in vivo* tests. We used the constructed EIF4A3 stable knockdown PC9 cell line to establish a nude mouse tumorigenic model. We used infected cells injected into the axillae of rats to construct a nude mouse tumorigenic model. The results showed that EIF4A3 knockdown dramatically reduced the tumor growth rate, tumor volume as well as tumor weight of nude mice (**Fig. 3A–C**). Subsequently, we used HE staining and IHC staining to confirm that the expression of EIF4A3

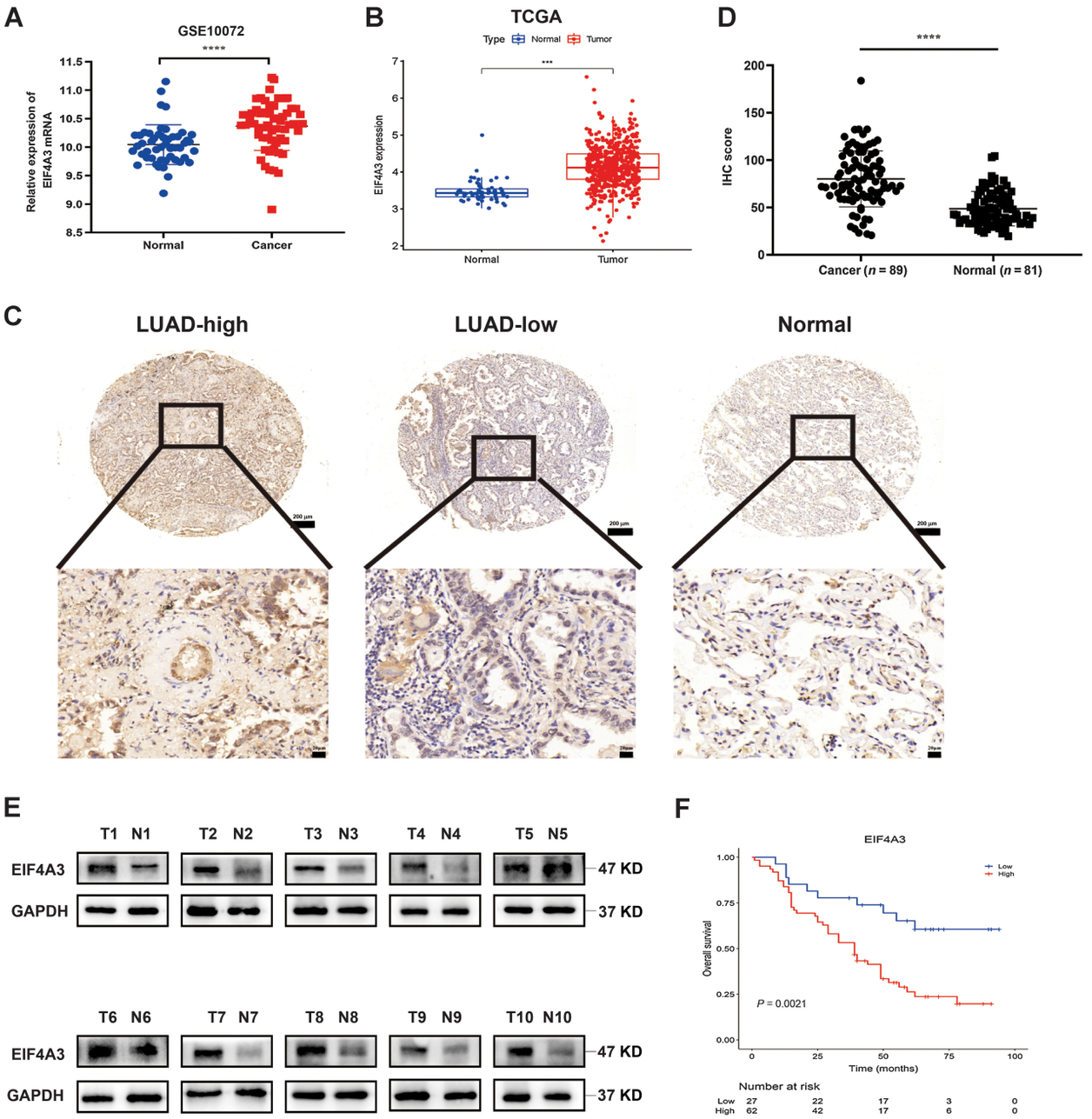

Figure 1.

Expression and prognostic of EIF4A3 in LUAD. **A** and **B,** EIF4A3 mRNA expression in LUAD and paracancerous tissues in GSE (GSE10072) and TCGA data sets. **C,** Representative IHC images of EIF4A3 expression of high expression and low expression in LUAD tissues and normal tissues. **D,** IHC score for EIF4A3 in the tissue microarray. **E,** EIF4A3 protein expression was detected by western blotting in 10 paired LUAD tissues. **F,** Kaplan–Meier analysis of LUAD cohorts based on a univariate analysis of survival using a log-rank statistical test. *, $P < 0.05$; **, $P < 0.01$; ***, $P < 0.001$; ****, $P < 0.0001$.

and proliferation index Ki67 was significantly reduced in the Sh-EIF4A3 group (**Fig. 3D**). Besides, we used infected cells for tail-vein injection in nude mice to construct a lung metastasis model. We photographed live nude mice removed lungs and livers from both groups by *in vivo* imaging and confirmed that knockdown of EIF4A3 markedly reduced LUAD cells' capacity to spread in the blood (**Fig. 3E** and **F**). Therefore, we found that not only *in vitro*, but also *in vivo*, knockdown EIF4A3 could inhibit the proliferation, migration, and invasion of LUAD cells.

FLOT1 was the downstream target of EIF4A3 in LUAD cells

Next, we wanted to explore the molecular action mechanism of EIF4A3 in LUAD. As no studies have so far focused on the ability of EIF4A3 to interact with other genes in lung cancer and thus exert its

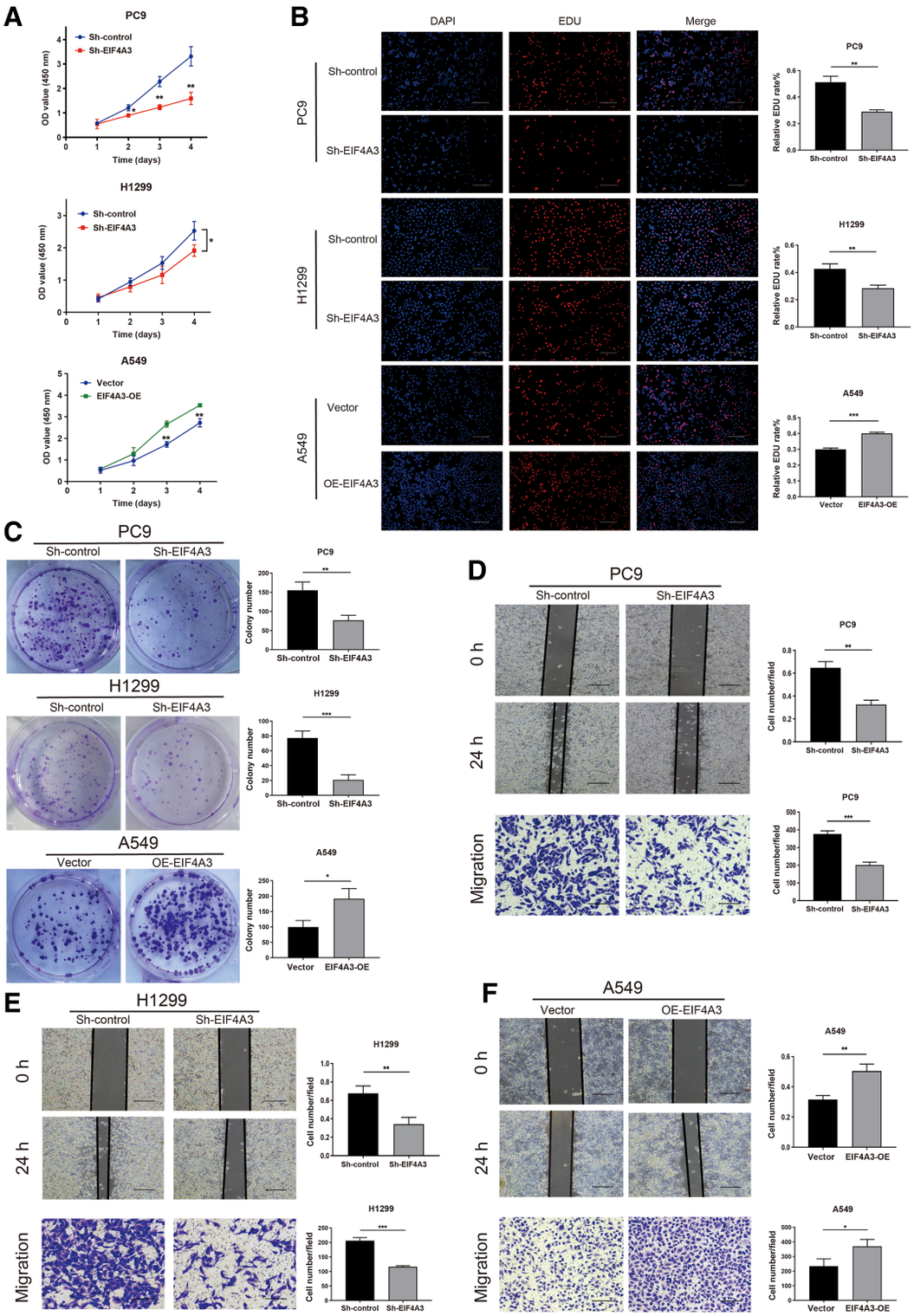

Figure 2.

EIF4A3 promotes LUAD cell proliferation and migration *in vitro*. **A–C,** CCK8 (**A**), EDU assay (**B**), and clone formation experiments (**C**) were performed to confirm the change of the proliferation ability after EIF4A3 knockdown in PC9 and H1299 cells and EIF4A3 expression in A549 cells. Scale bar of EDU assay: 200 μm. **D–F,** Wound healing and transwell migration experiment without matrigel were performed to identify the change of migration ability after EIF4A3 knockdown in PC9 cells (**D**) and H1299 cells (**E**) and EIF4A3 overexpression in A549 cells (**F**). Scale bar of wound healing experiment: 500 μm. Scale bar of transwell migration experiment: 200 μm. All data are presented as the mean ± SD. $n = 3$. *, $P < 0.05$; **, $P < 0.01$; ***, $P < 0.001$; ****, $P < 0.0001$.

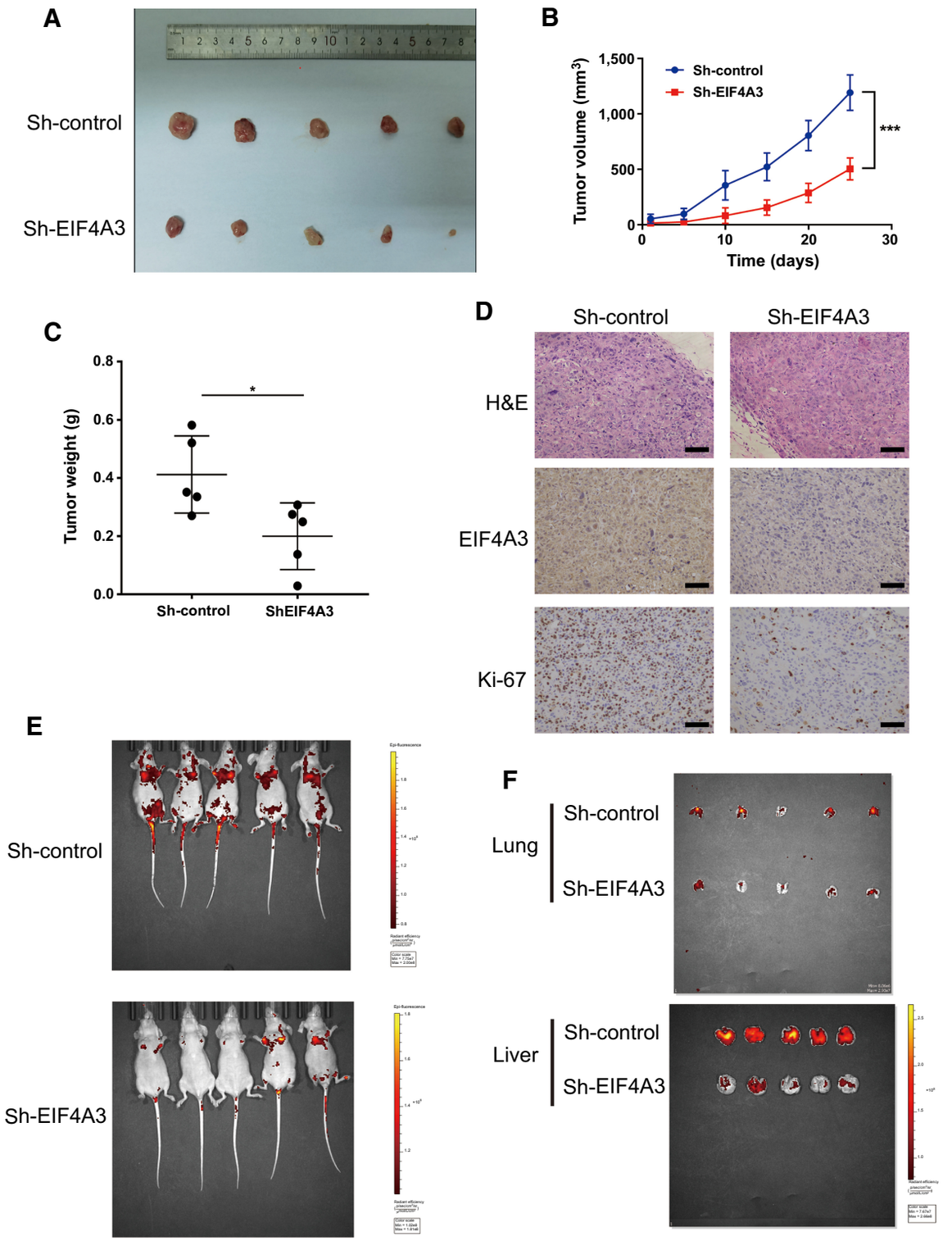

Figure 3.

EIF4A3 promotes LUAD cell proliferation and metastasis *in vivo*. **A,** Representative images of tumors in nude mice from different treatment groups 5 weeks after tumor injection. **B** and **C,** The volume (**B**) and the weight were lower for xenograft tumors with EIF4A3 knockdown than for xenograft tumors with negative control. **D,** Representative images of HE staining and IHC staining of EIF4A3 and Ki-67 in xenograft tumors. Scale bar, 100 μm. **E,** The metastasis of LUAD cells in the EIF4A3 knockdown group was significantly lower in nude mice than in the control group using *in vivo* imaging of live nude mice. **F,** Representative images of lung metastasis and liver metastasis from different treatment groups using *in vivo* imaging of isolated organs. *, $P < 0.05$; **, $P < 0.01$; ***, $P < 0.001$; ****, $P < 0.0001$.

procancer effects. Therefore, we decided to explore and search for the target partners of EIF4A3 and their interactions. To find them, we performed immunoprecipitation and subjected the eluted bead precipitates to proteomic analysis and mass spectrometry. After the exclusion of some ribosomal proteins and heavy-chain proteins, we then obtained proteins that may interact with EIF4A3, from which we selected Flotillin-1, a gene that had been reported to affect the progression of LUAD (19). Subsequently, we selected H1299 and PC9 cell lines with high expression of EIF4A3 to verify whether endogenous EIF4A3 can interact with Flotillin-1 and endogenous Flotillin-1 can interact with EIF4A3. The results showed that EIF4A3 was able to interact with Flotillin-1 (**Fig. 4A**). We then performed the IHC staining of tumors formed by infected LUAD cells in nude mice and found that the knockdown of EIF4A3 resulted in downregulation of FLOT1 expression in tumor tissues (**Fig. 4B**). At the same time, the relative expression of EIF4A3 and FLOT1 showed that the reduction of EIF4A3 in LUAD cells led to a decrease in FLOT1 expression, whereas FLOT1 expression was upregulated as a result of EIF4A3 overexpression (**Fig. 4D–G**). We then performed the determination of the basal expression of FLOT1 in two lung normal epithelial cells and four LUAD cell lines, which guided the establishment of the FLOT1-knockdown PC9 cells using two siRNA sequences to perform subsequent experiments (Supplementary Fig. S1D). In addition to verifying the knockdown efficiency of the two sequences, we also found that the knockdown of FLOT1 in LUAD cell lines had no effect on the expression of EIF4A3 (Supplementary Fig. S1E and S1F). These findings suggested that EIF4A3 could positively regulate FLOT1 expression, whereas FLOT1 did not alter the expression of EIF3A3. Taken together, Flotillin-1 is a downstream target gene of EIF4A3.

EIF4A3 induces LUAD cell tumorigenesis through the PI3K–AKT–ERK1/2–P70S6K pathway

Next, we performed transcriptome sequencing in order to find a clear pathway through which EIF4A3 affects LUAD development. Pathway enrichment revealed that EIF4A3 may be most associated with the Apelin pathway in addition to some pathways unrelated to tumor development (**Fig. 4C**). It has been demonstrated that the Apelin pathway is closely linked to the development of tumors, including lung cancer (20–22). Besides, the downstream gene of EIF4A3, FLOT1 had been reported to be associated with PI3K–AKT–ERK–P70S6K pathway (23), which was included in the apelin signaling pathway. Therefore, we selected these tumor-related genes downstream of the Apelin pathway to verify the effect of EIF4A3 on the PI3K–AKT–ERK1/2–P70S6K pathway, which were also essential for many activities of cancer. The western blotting showed that EIF4A3 was positively related to the expression of PI3K, phosphorylated AKT, and phosphorylated ERK and P70S6K in the pathway (**Fig. 4D–F**).

EIF4A3 promotes PI3K class III–mediated autophagy

The process through which cells recycle cytoplasm and defective organelles in response to stressors such as nutrient deficiency is called autophagy (24). Autophagy has a two-sided effect on tumor development, whereas different levels of autophagy can lead tumors to different courses and autophagy has been reported to be altered in LUAD (25, 26). The Apelin pathway not only includes the PI3K–AKT–ERK1/2–P70S6K pathway but also includes the type III PI3K, which can activate autophagy (**Fig. 5E**), and we confirmed in the previous experiment that EIF4A3 can positively regulate the PI3K–AKT–ERK–P70S6K pathway, so it is a question of interest whether EIF4A3 can affect autophagy in LUAD. The results of transmission electron microscopy demonstrated that EIF4A3 knockdown lowered the amount of intracellular autophagic vesicles and autophagic lysosomes, whereas overexpression of EIF4A3 did the opposite (**Fig. 5A**). For further validation, we selected several autophagy-related genes. Western blotting demonstrated that the knockdown of EIF4A3 could downregulate the expression of Beclin-1, LC3A/B, Atg5, Atg3, Atg7, Atg16L1, and Atg12 and upregulate the expression of P62, whereas overexpression of EIF4A3 did the opposite (**Fig. 5B–D**). These results demonstrated that EIF4A3 could mediate autophagy.

FLOT1 plays a role in cancer promotion in LUAD and is also related to poor prognosis in LUAD patients

Although FLOT1 has been reported in the literature to contribute to the development of LUAD (19), we performed a simple experimental validation. At first, we performed the bioinformatic analysis to demonstrate this result. With GEO LUAD databases (GSE10072) and TCGA LUAD database, FLOT1 expression was observed to be greater in LUAD tissues than in normal tissues (**Fig. 6A** and **B**). Apart from this, high FLOT1 expression was significantly correlated with a poor prognosis in LUAD according to Kaplan–Meier survival analysis from the Kaplan–Meier Plotter online website (**Fig. 6C**). Subsequently, we evaluated the prognosis of patients with high EIF4A3 expression and high FLOT1 expression using the TCGA database which was downloaded from UCSC Xena. The results revealed that patients with high EIF4A3 expression and high FLOT1 expression had a worse prognosis compared with other patients (Supplementary Fig. S1G). Based on previous experiments, we selected the PC9 cell line as well as two interfering sequences of FLOT1 for *in vitro* experiments, we then found that knockdown of FLOT1 lowered PC9 cell proliferative rate and migratory ability (**Fig. 6D–G**). These findings confirmed that FLOT1 performed a protumor role in LUAD and was closely correlated with patient prognosis.

EIF4A3 activated the apelin signaling pathways through flotillin-1 in LUAD cells

In previous experiments, we demonstrated that EIF4A3 and FLOT1 can influence tumor progression by affecting the Apelin pathway. To verify whether Flotillin-1 is involved in the mechanism by which EIF4A3 affects lung cancer progression, we performed rescue experiment. Because of the positive correlation between EIF4A3 and Flotillin-1 in LUAD, we chose to perform experiments with one of the siRNA-FLOT1's sequences transfected in a preestablished A549 cell line with stable overexpression of EIF4A3. We found that Flotillin-1 knockdown significantly reduced the upregulation of the PI3K–AKT–ERK–P70S6K pathway and autophagy pathway-related protein expression induced by EIF4A3 overexpression (**Fig. 7E**) and reduced the increase in proliferation and migration capacity of LUAD cells induced by EIF4A3 overexpression (**Fig. 7A–D**). These results suggested that Flotillin-1 played an important role in the cancer-promoting effect and molecular mechanism of EIF4A3.

Discussion

This study elucidates the molecular role of the translation initiation factor EIF4A3 can play a pro-oncogenic role in LUAD through its downstream target gene FLOT1. We found not only that the expression of EIF4A3 was widely high in LUAD tissues but also that a high level of EIF4A3 expression was tied to the patients with a bad prognosis. Meanwhile, we proved that the level of EIF4A3 protein expression was substantially associated with the TNM stage and tumor size. In addition, we found that EIF4A3 could promote tumor proliferation and migration *in vitro* and *in vivo*. In summary, EIF4A3 may

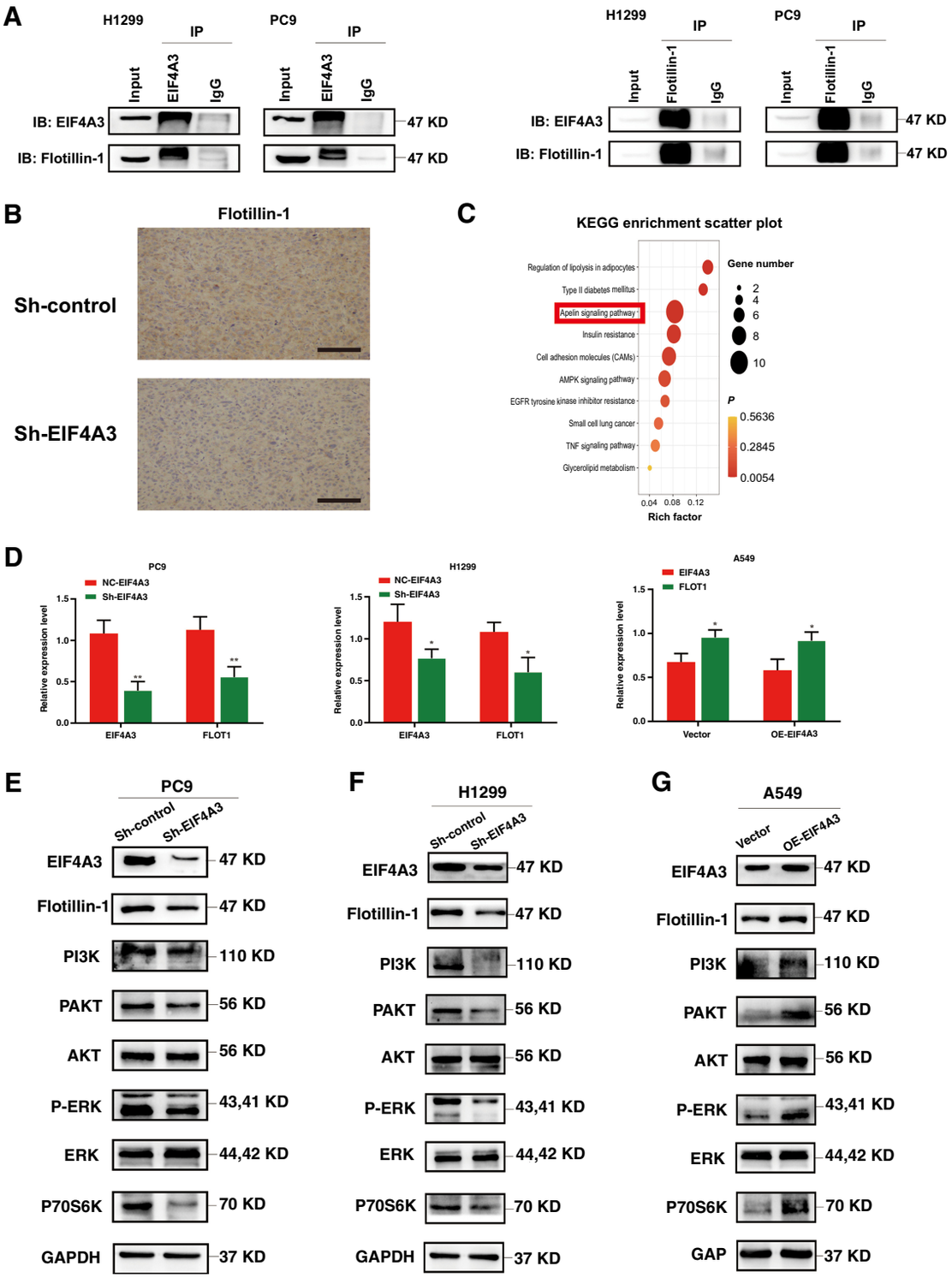

Figure 4.
EIF4A3 can regulate the expression of its downstream target gene Flootillin-1 and affect PI3K–AKT–ERK1/2–P70S6K pathway in LUAD cells. **A,** Immunoprecipitation in PC9 and H1299 cell lines confirmed the ability of EIF4A3 to interact with Flotillin-1 after the addition of antibodies to EIF4A3 and Flotillin-1. **B,** Representative images of IHC staining of FLOT1 in xenograft tumors from the EIF4A3 knockdown treatment group and negative control group. Scale bar, 100 μm. **C,** Signaling pathways of altered genes after EIF4A3 knockdown in PC9 cells using KEGG pathway enrichment after performing transcriptomic sequencing. Statistical significance is indicated by different colors. The size of the circle represents the number of genes. **D,** Relative expression of EIF4A3 and Flotillin-1 after knockdown and overexpression of EIF4A3 in three cell lines. **E–G,** Flotillin-1 and PI3K–AKT–ERK1/2–P70S6K pathway expression was regulated by EIF4A3.

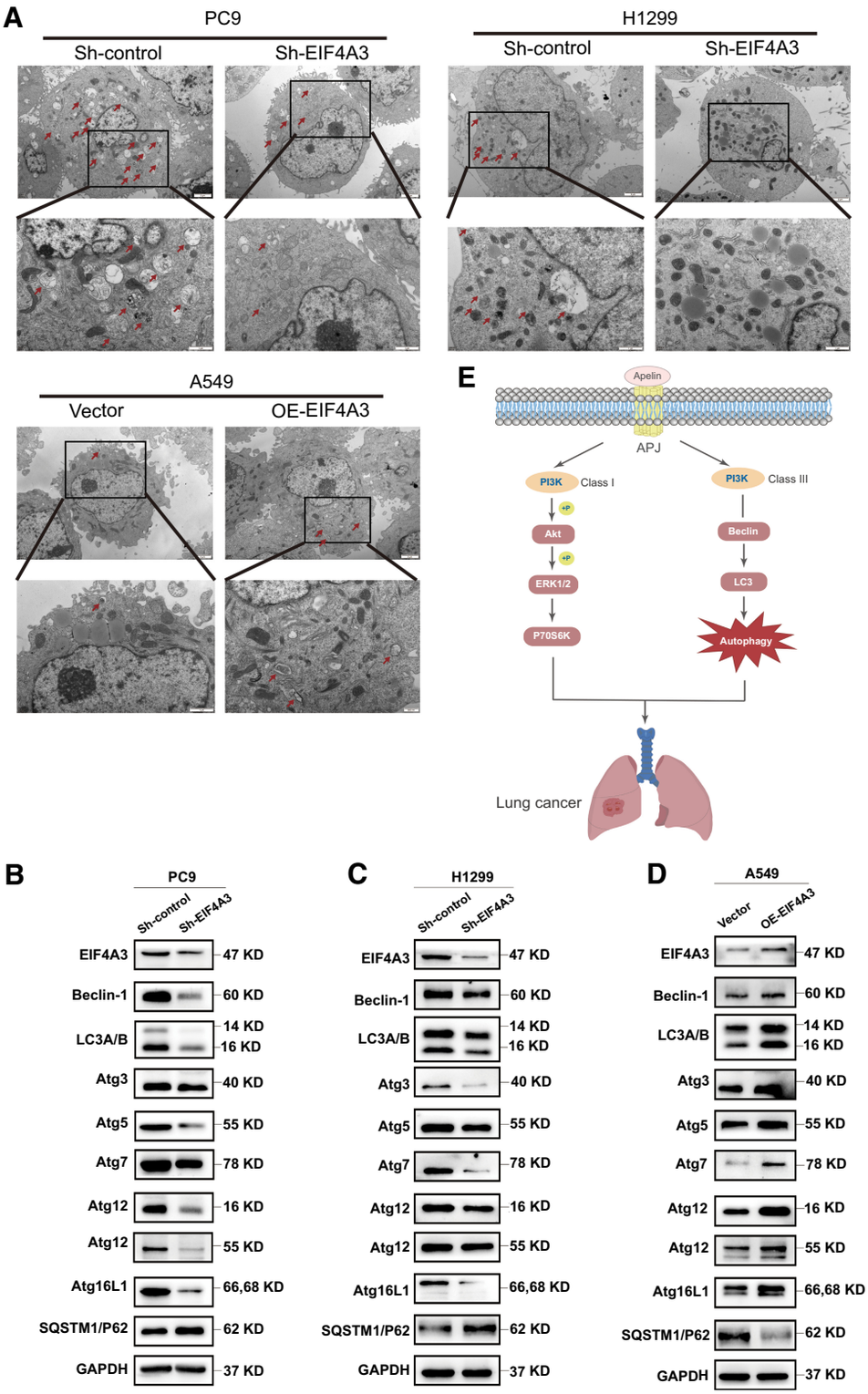

Figure 5.

EIF4A3 can activate PI3K class III–mediated autophagy in LUAD cells. **A,** Transmission electron microscopy was performed to confirm the changes in the number of autophagic vesicles and autophagic lysosomes after EIF4A3 knockdown in PC9 and H1299 cells and EIF4A3 expression in A549 cells. **B–D,** Autophagy-related genes Beclin-1, LC3A/B, Atg7, Atg5, Atg3, Atg12, Atg16L1, and P62 were regulated by EIF4A3 after related treatment in PC9 (**B**), H1299 (**C**), and A549 (**D**) cells. **E,** The pathways that EIF4A3 affects in the Apelin pathway in LUAD.

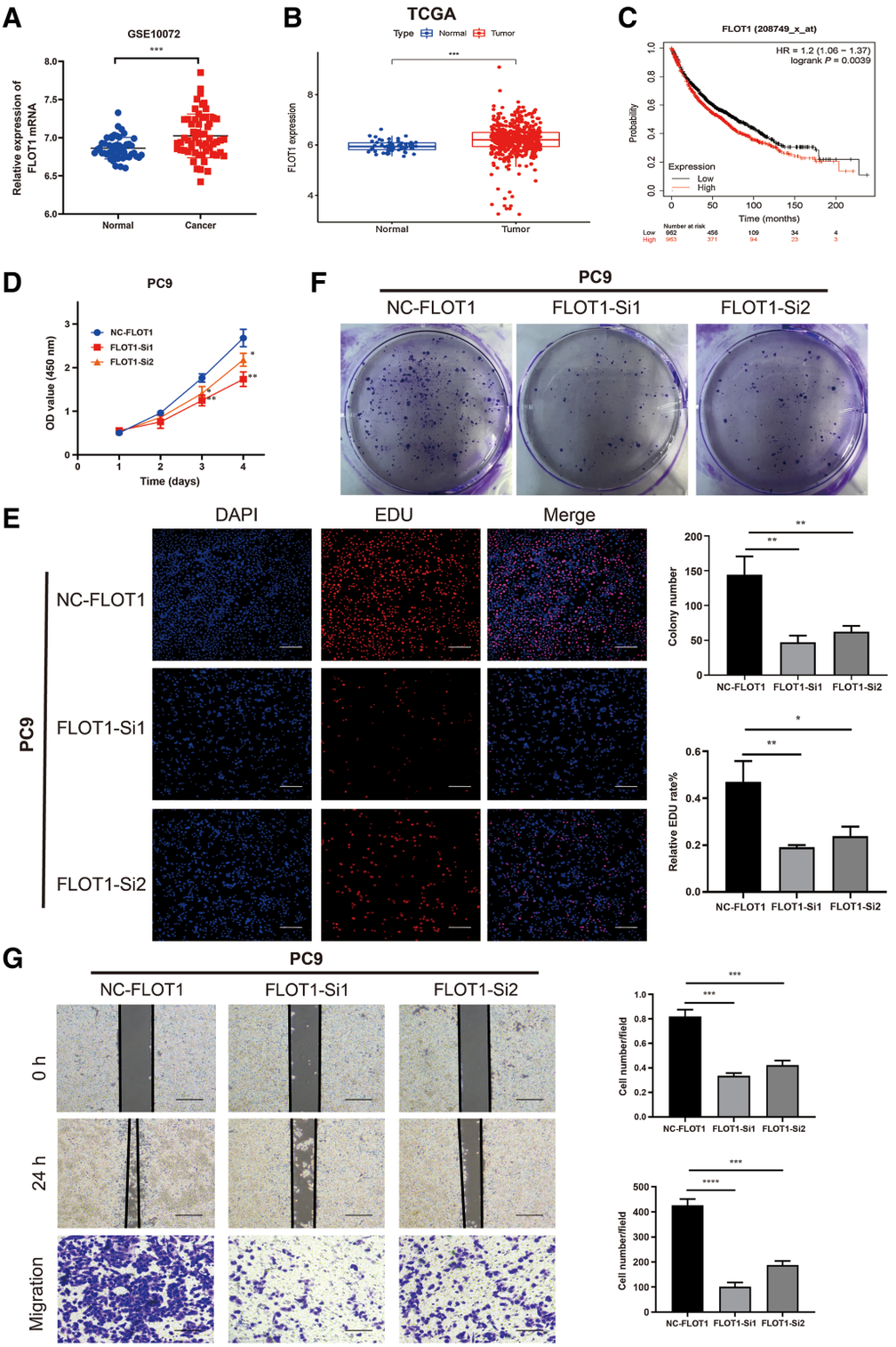

Figure 6.

Flotillin-1 plays a procarcinogenic role in LUAD. **A** and **B,** FLOT1 mRNA expression in LUAD and paracancerous tissues in GSE (GSE10072; **A**) and TCGA (**B**) data sets. **C,** Online Kaplan–Meier analysis of LUAD cohorts based on univariate analysis of survival using a log-rank statistical test. **D–F,** CCK8 (**D**), EDU assay (**E**), and clone formation experiments (**F**) were performed to confirm the change of the proliferation ability after FLOT1 knockdown in PC9 cells. All data are presented as the mean ± SD. $n = 3$. **G,** Wound healing and transwell migration experiments without matrigel were performed to identify the change of migration ability after FLOT1 knockdown in PC9 cells. All data are presented as the mean ± SD. $n = 3$. *, $P < 0.05$; **, $P < 0.01$; ***, $P < 0.001$; ****, $P < 0.0001$.

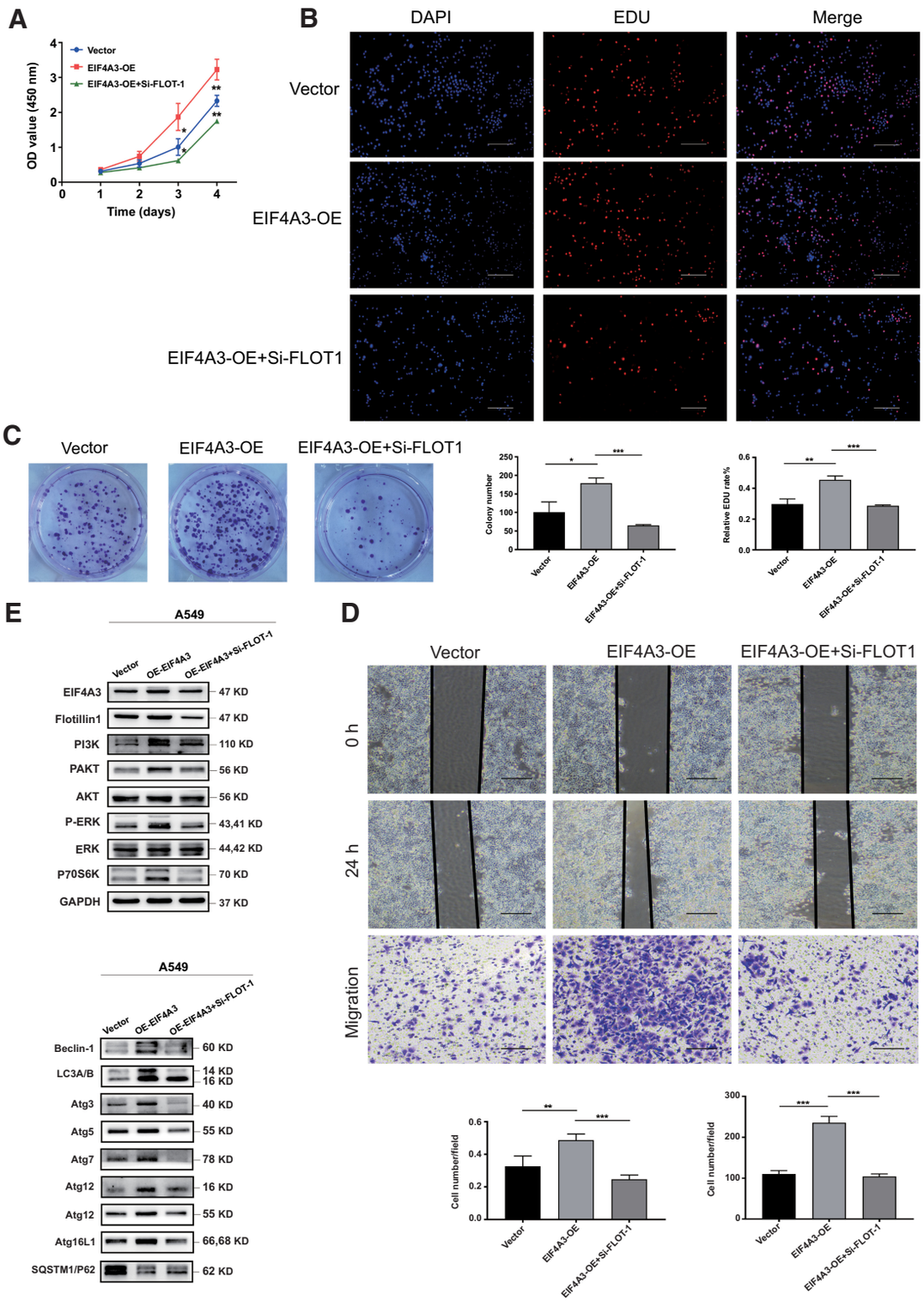

Figure 7.

EIF4A3 activates the apelin pathways through Flotillin-1. **A–C,** CCK8 (**A**), EDU assay (**B**), and clone formation experiments (**C**) of the rescue experiment were performed to confirm the change of the proliferation ability in A549 cells. Data are presented as the mean ± SD. $n = 3$. **D,** Wound healing and transwell migration assay without matrigel of the rescue experiment were performed to identify the change of migration ability in A549 cell. Data are presented as the mean ± SD. $n = 3$. **E,** Western blot analysis of PI3K–AKT–ERK1/2–P70S6K signaling pathways and autophagy-related markers of the rescue experiment in A549 cell. *, $P < 0.05$; **, $P < 0.01$; ***, $P < 0.001$; ****, $P < 0.0001$.

be a potential biomarker and therapeutic target for LUAD and can predict patient prognosis.

Through proteomics sequencing and mass spectrometry analysis, our study identified possible downstream target genes that interacted with EIF4A3, which we subsequently combined with the significance of these genes in lung cancer and immunoprecipitation validation. Fortunately, the immunoprecipitation results showed that EIF4A3 was able to interact with FLOT1, an oncogenic gene in lung cancer. Subsequently, the results of IHC staining and western blotting confirmed that EIF4A3 was able to positively modulate the expression of FLOT1. In addition, the knockdown of FLOT1 was able to reduce the elevated proliferation and migration ability of LUAD cells in response to EIF4A3 overexpression, which also provided sufficient evidence to confirm that FLOT1 is a downstream target gene of EIF4A3 in LUAD.

Our study confirms that the downstream target gene FLOT1 plays a procancer role in LUAD. FLOT1, a Flotillin protein family member, is essential for numerous cellular activities and transduction of cellular signals (27). Previous research has demonstrated that the sequences of amino acids in flotillin-1 and flotillin-2 are approximately 44% same among some species, and up to 99% identical between mice and humans, indicating that flotillins have been extensively conserved in evolution (28). Meanwhile, EIF4A3 also has a conserved DEAD–BOX structural domain, which also provides a possible binding site for their binding. The human flotillin-1 gene is a 15-kb single-copy housekeeping gene with 13 exons and 12 introns (29), which is also highly expressed in a variety of tumors. Sumoylation of FLOT1 can promote the migration and invasion of prostate cancer (30), and FLOT1 can be regulated by microRNAs to affect breast cancer (31). More importantly, FLOT1 has been reported to affect the migration and proliferation of lung cancer through the TGFβ pathway and the ERK/AKT pathway (23, 32), which lays the foundation for their joint tumor-promoting effects.

Our findings also show that EIF4A3 can activate the Apelin signaling pathway via FLOT1 in LUAD. With transcriptome sequencing and possible pathways of action of the downstream target gene FLOT1 that have been reported (23), we speculate that EIF4A3 may affect LUAD development by activating the Apelin signaling pathway. Meanwhile, in the Apelin signaling pathway, we selected two pathways: PI3K–AKT-ERK1/2-P70S6K pathway and PI3K class III–mediated autophagy pathway, which could play the same role in cellular life activities. Using western blotting, we found that EIF4A3 could positively regulate the expression of PI3K, PAKT, PERK, and P70S6K. Using TEM and western blotting, we found EIF4A3 could promote autophagy in LUAD cells. In addition, we found that the knockdown of FLOT1 reversed the carcinogenic effect of EIF4A3 overexpression and the Apelin pathway activated by EIF4A3 overexpression. In conclusion, our study demonstrates that EIF4A3 can affect lung cancer progression by activating the Apelin pathway through FLOT1.

It is well known that autophagy is a double-edged sword, which may play different roles in different tumors as well as different stages of tumors. In this experiment, we confirmed that EIF4A3 can promote CLASS III-mediated autophagy in LUAD. Whereas it has been reported in the literature that EIF4A3 can function as an autophagy gatekeeper in some tumors (33), it has also been reported that EIF4A3 has a positive correlation with some autophagy-related genes (34). Are such different roles present in different stages of tumors? Or are the pathways and mechanisms affecting autophagy different? This also needs to be studied in depth. Other than that, we still have many questions that we need to follow up on with in-depth research. At first, how does EIF3A3 upregulate the expression of its downstream target gene FLOT1? Most studies now mention that EIF4A3 plays a role as an RNA-binding protein regulating RNA, but few studies mention that it affects protein expression. Therefore, an in-depth study on how EIF4A3 upregulates FLOT1 expression, whether through, for example, inhibition of ubiquitination, remains to be followed. Second, where is the specific binding site of EIF4A3 to FLOT1? In 1999, EIF4A3 and its predicted gene were found (35). The structure of EIF4A3 resembles a dumbbell, with two compact domains joined by a flexible linker and it contains a DEAD-box domain and a Q domain (11, 36), whereas FLOT1 is a 15-kb housekeeping gene with a single copy. So the two structural domains of EIF4A3 are the key to determining the specific binding sites of the two genes. We will also learn and adopt appropriate methods to explore the binding domain of EIF4A3 in the long run.

In conclusion, we reported an oncogene, EIF4A3, in lung cancer that could promote LUAD progression through the Apelin signaling pathway by regulating a downstream target gene, FLOT1, and can also affect the prognosis of lung cancer patients. Our study will also provide new potential therapeutic goals for patients with LUAD and contribute to the improvement of poor patient prognosis.

Authors' Disclosures

No disclosures were reported.

Authors' Contributions

W. Yu: Conceptualization, formal analysis, visualization, methodology, writing–original draft. **J. Liang:** Conceptualization, validation, writing–review and editing. **T. Fang:** Writing–review and editing. **J. Jiang:** Writing–review and editing. **R. Zhao:** Resources. **R. Li:** Resources. **J. Han:** Data curation. **H. Tian:** Conceptualization, supervision, funding acquisition, project administration, writing–review and editing.

Acknowledgments

This study was financially supported by the Shandong Provincial Natural Science Foundation of China (No. ZR2021LSW006) and the Taishan Scholar Program of Shandong Province (No. ts201712087).

The publication costs of this article were defrayed in part by the payment of publication fees. Therefore, and solely to indicate this fact, this article is hereby marked "advertisement" in accordance with 18 USC section 1734.

Note

Supplementary data for this article are available at Molecular Cancer Research Online (http://mcr.aacrjournals.org/).

Received December 12, 2022; revised February 27, 2023; accepted March 29, 2023; published first April 3, 2023.

References

1. Bade BC, Dela Cruz CS. Lung cancer 2020. Clin Chest Med 2020;41:1–24.
2. Travis WD, Brambilla E, Nicholson AG, Yatabe Y, Austin JHM, Beasley MB, et al. The 2015 World Health Organization classification of lung tumors. J Thorac Oncol 2015;10:1243–60.
3. Hirsch FR, Scagliotti GV, Mulshine JL, Kwon R, Curran WJ, Wu Y-L, et al. Lung cancer: current therapies and new targeted treatments. Lancet North Am Ed 2017;389:299–311.
4. Lemjabbar-Alaoui H, Hassan OU, Yang Y-W, Buchanan P. Lung cancer: biology and treatment options. Biochim Biophys Acta 2015;1856:189–210.
5. Naylor EC, Desani JK, Chung PK. Targeted therapy and immunotherapy for lung cancer. Surg Oncol Clin N Am 2016;25:601–9.
6. Alexander M, Kim SY, Cheng H. Update 2020: management of non-small cell lung cancer. Lung 2020;198:897–907.

7. Raza F, Waldron JA, Quesne JL. Translational dysregulation in cancer: eIF4A isoforms and sequence determinants of eIF4A dependence. Biochem Soc Trans 2015;43:1227–33.
8. Chu J, Pelletier J. Targeting the eIF4A RNA helicase as an anti-neoplastic approach. Biochim Biophys Acta 2015;1849:781–91.
9. Tillotson J, Kedzior M, Guimarães L, Ross AB, Peters TL, Ambrose AJ, et al. ATP-competitive, marine derived natural products that target the DEAD box helicase, eIF4A. Bioorg Med Chem Lett 2017;27:4082–5.
10. Lu W-T, Wilczynska A, Smith E, Bushell M. The diverse roles of the eIF4A family: you are the company you keep. Biochem Soc Trans 2014;42:166–72.
11. Ye J, She X, Liu Z, He Z, Gao X, Lu L, et al. Eukaryotic initiation factor 4A-3: a review of its physiological role and involvement in oncogenesis. Front Oncol 2021;11:712045.
12. Zheng X, Huang M, Xing L, Yang R, Wang X, Jiang R, et al. The circRNA circSEPT9 mediated by E2F1 and EIF4A3 facilitates the carcinogenesis and development of triple-negative breast cancer. Mol Cancer 2020;19:73.
13. Wang X, Chen M, Fang L. hsa_circ_0068631 promotes breast cancer progression through c-Myc by binding to EIF4A3. Mol Ther Nucleic Acids 2021;26:122–34.
14. Jiang X, Guo S, Wang S, Zhang Y, Chen H, Wang Y, et al. EIF4A3-induced circARHGAP29 promotes aerobic glycolysis in docetaxel-resistant prostate cancer through IGF2BP2/c-Myc/LDHA signaling. Cancer Res 2022;82:831–45.
15. Wei Y, Lu C, Zhou P, Zhao L, Lyu X, Yin J, et al. EIF4A3-induced circular RNA ASAP1 promotes tumorigenesis and temozolomide resistance of glioblastoma via NRAS/MEK1/ERK1-2 signaling. Neuro-oncol 2021;23:611–24.
16. Jiang Z, Tai Q, Xie X, Hou Z, Liu W, Yu Z, et al. EIF4A3-induced circ_0084615 contributes to the progression of colorectal cancer via miR-599/ONECUT2 pathway. J Exp Clin Cancer Res 2021;40:227.
17. Li N, Zhan X. Anti-parasite drug ivermectin can suppress ovarian cancer by regulating lncRNA-EIF4A3-mRNA axes. EPMA J 2020;11:289–309.
18. Takahashi S, Noro R, Seike M, Zeng C, Matsumoto M, Yoshikawa A, et al. Long non-coding RNA CRNDE is involved in resistance to EGFR tyrosine kinase inhibitor in EGFR-mutant lung cancer via eIF4A3/MUC1/EGFR signaling. IJMS 2021;22:4005.
19. Guo AY, Liang XJ, Liu RJ, Li XX, Bi W, Zhou LY, et al. Flotilin-1 promotes the tumorigenicity and progression of malignant phenotype in human lung adenocarcinoma. Cancer Biol Ther 2017;18:715–22.
20. Yan J, Wang A, Cao J, Chen L. Apelin/APJ system: an emerging therapeutic target for respiratory diseases. Cell Mol Life Sci 2020;77:2919–30.
21. Dogra S, Neelakantan D, Patel MM, Griesel B, Olson A, Woo S. Adipokine apelin/APJ pathway promotes peritoneal dissemination of ovarian cancer cells by regulating lipid metabolism. Mol Cancer Res 2021;19:1534–45.
22. Chaves-Almagro C, Auriau J, Dortignac A, Clerc P, Lulka H, Deleruyelle S, et al. Upregulated apelin signaling in pancreatic cancer activates oncogenic signaling pathways to promote tumor development. IJMS 2022;23:10600.
23. Zhang L, Mao Y, Mao Q, Fan W, Xu L, Chen Y, et al. FLOT1 promotes tumor development, induces epithelial–mesenchymal transition, and modulates the cell cycle by regulating the Erk/Akt signaling pathway in lung adenocarcinoma. Thorac Cancer 2019;10:909–17.
24. Hu G, Hacham M, Waterman SR, Panepinto J, Shin S, Liu X, et al. PI3K signaling of autophagy is required for starvation tolerance and virulence of cryptococcus neoformans. J Clin Invest 2008;118:1186–97.
25. Jiang G-M, Tan Y, Wang H, Peng L, Chen H-T, Meng X-J, et al. The relationship between autophagy and the immune system and its applications for tumor immunotherapy. Mol Cancer 2019;18:17.
26. Liu G, Pei F, Yang F, Li L, Amin A, Liu S, et al. Role of autophagy and apoptosis in non-small-cell lung cancer. IJMS 2017;18:367.
27. Langhorst MF, Reuter A, Stuermer CAO. Scaffolding microdomains and beyond: the function of reggie/flotillin proteins. Cell Mol Life Sci 2005;62:2228–40.
28. Schulte T, Paschke KA, Laessing U, Lottspeich F, Stuermer CAO. Reggie-1 and reggie-2, two cell surface proteins expressed by retinal ganglion cells during axon regeneration. Development 1997;124:577–87.
29. Edgar AJ, Polak JM. Flotillin-1: gene structure: cDNA cloning from human lung and the identification of alternative polyadenylation signals. Int J Biochem Cell Biol 2001;33:53–64.
30. Jang D, Kwon H, Choi M, Lee J, Pak Y. Sumoylation of Flotillin-1 promotes EMT in metastatic prostate cancer by suppressing Snail degradation. Oncogene 2019;38:3248–60.
31. Li L, Luo J, Wang B, Wang D, Xie X, Yuan L, et al. Microrna-124 targets flotillin-1 to regulate proliferation and migration in breast cancer. Mol Cancer 2013;12:163.
32. Lianmei Z, Jie L, Yueping L, Wei Z, Yanan S, Xinyi F, et al. Flotillin1 promotes EMT of human small cell lung cancer via TGF-β signaling pathway. Cancer Biology & Medicine 2018;15:400.
33. Sakellariou D, Frankel LB. EIF4A3: a gatekeeper of autophagy. Autophagy 2021;17:4504–5.
34. Yu F, Zhang Y, Wang Z, Gong W, Zhang C. Hsa_circ_0030042 regulates abnormal autophagy and protects atherosclerotic plaque stability by targeting eIF4A3. Theranostics 2021;11:5404–17.
35. Holzmann K, Gerner C, Pöltl A, Schäfer R, Obrist P, Ensinger C, et al. A human common nuclear matrix protein homologous to eukaryotic translation initiation factor 4A. Biochem Biophys Res Commun 2000;267:339–44.
36. Budiman ME, Bubenik JL, Driscoll DM. Identification of a signature motif for the eIF4a3–SECIS interaction. Nucleic Acids Res 2011;39:7730–9.